Lewis Number Effects on Lean Premixed Combustion Characteristics of Multi-Component Fuel Blends

Authors: Zitouni, S. (*), Pugh D., Crayford A., Bowen, P.J., Runyon, J.

Cardiff University, School of Engineering & The Gas Turbine Research Centre (GTRC)

(*) Corresponding Author Email:

ZitouniSM@cardiff.ac.uk

Address:

W 1.32, Queen's Buildings, 14-17 The Parade, Cardiff CF24 3AA, United Kingdom

Abstract:

Variation in natural gas composition, alongside the potential for H_2 enrichment, creates the potential for significant changes to premixed flame behaviour. To strengthen fundamental understanding of lean multi-component alternative fuel blends, an outwardly propagating spherical flame was employed to measure the flame speeds and Markstein lengths of C_1-C_4 hydrocarbons, alongside precisely mixed blends of CH_4/C_2H_6, CH_4/C_3H_8 and CH_4/H_2. Theoretical relationships between Markstein length and Lewis Number are explored alongside effective Lewis number formulations. Under lean conditions, equal volumetric additions of H_2 and C_3H_8 (30% vol.) to CH_4 resulted in similar augmentation of burning velocity, however, opposite susceptibility to preferential diffusional instability was noted. At a fixed equivalence ratio of 0.65, limited changes in composition provide a marked change in the premixed flame response with the addition of C_2H_6 and C_3H_8 to CH_4. For lean CH_4/H_2 mixtures, a diffusional based Lewis Number formulation yielded a favourable correlation, whilst a heat-release model resulted in better agreement for lean CH_4/C_3H_8 blends. Modelling work suggests that measured enhancement of lean CH_4 flames upon H_2 or C_3H_8 is strongly correlated to changes in volumetric heat release rates and production of H radicals. Furthermore, a systematic analysis of the flame speed enhancement effects (thermal, kinetic, diffusive) of H_2 and C_3H_8 addition to methane was undertaken. Augmented flame propagation of CH_4/H_2 and CH_4/C_3H_8 was demonstrated to be principally an Arrhenius effect, predominantly through reduction of associated activation energy. Finally, plausible short-term variations in composition with hydrogen-enriched multi-component natural gas flames were investigated experimentally and numerically. At the leanest conditions, small variations in CH_4:C_3H_8 content at a fixed H_2 fraction resulted in discernible changes in stretch related behaviour, a reflection of the thermo-diffusive behaviour of each fuel's response.

Key words: Laminar flame Speed, Lewis Number, Markstein Length, Fuel Mixtures, Hydrogen, Natural Gas

1.Introduction

Natural gas composition varies significantly, depending on source location, extraction, and refinement process [1]. Methane (CH_4) levels have been shown to fluctuate between 55.8% to 98.1%, with concentrations of higher hydrocarbons (C_2+), typically ethane (C_2H_6) and propane (C_3H_8), varying from 0.5% - 13.3% and 0% - 23.7%, respectively [2]. Hydrogen (H_2) blending, sourced from various waste and sustainable processes, has also been proposed towards decarbonised gas networks. With the growing share of renewable energy sources, coupled with the demand of high-efficiency and low-emission power plants, combustor flexibility is of increasing importance in meeting the dynamic requirements of power generation systems, in terms of load and fuel variations [3]. Variations in natural gas composition and potential H_2 enrichment presents significant combustion challenges to power generation gas turbines [4], particularly those running near the lean-limit, as this combustion regime tends to exacerbate any variation in flame behaviour, potentially leading to flame instability or extinction [5]. As such, there seems to be a practical necessity to develop and strengthen understanding of fundamental combustion characteristics of lean multi-component fuel blends, ultimately leading to the development of combustors tolerant of an increased share of either H_2 and/or C_2+ gases.

Fuel composition variation introduces changes in chemical and transport properties, which in turn alters the witnessed reactivity and burning characteristics of the fuel mixture. The Lewis number (Le), defined as the ratio of thermal to mass diffusivity of the deficient reactant, represents a key property in premixed combustion systems, detailing the transport mechanisms of various species across the flame front. For stretched flames – undergoing the combined effects of strain, curvature, and flame motion – preferential diffusion (i.e., Le diverging from unity) is understood to strongly influence the burning rates of premixed flames [6]. Thermo-diffusively unstable flames with Le < 1 show a relative acceleration with increasing stretch rate, whereas conversely for flames exhibiting Le > 1 there is greater relative thermal diffusivity, resulting in heat loss to the unburned reactants and a reduction in burning rate with increased stretch [7]. This effect is also observed at increased turbulence intensity with Le < 1 mixtures exhibiting a greater increase in burning rate for an equivalent rise in turbulent velocity fluctuation [8]. A parameter often measured to characterise the influence of Le on the change in flame speed with stretch rate is the burned gas Markstein length (L_b). Markstein number - defined as L_b divided by the flame thickness (δ) - is an indicator of the propensity of a combustion system to be influenced by thermo-acoustic instability [9], and is thus of interest to study.

Lipatnikov and Chomiak [6], in their extensive review of molecular transport effects on flame propagation and structure, underline that weak and strong turbulent premixed combustion is affected by preferential diffusional instabilities, with increased turbulence resulting in enhanced wrinkling of the flame front, which in turn increases the turbulent burning rate [10]. However, diffusive effects in turbulent flames are often overlooked in simplified numerical simulations. Such simplification is not problematic in the case of the quasi equi-diffusive lean CH_4/air mixtures. However, issues potentially arise with increased concentrations of alternative fuels which has led to increased interest in this field [3,10–13]. Recent DNS studies characterised the influence of Le for a range of pure and blended fuels (H_2, CH_4 and C_3H_8) demonstrating an amplification of the diffusive effects, according to each fuels' Le behaviour [8,10,12,14]. Experimental validation of these findings is limited, with some studies investigating fixed compositions of natural gas or blends of CH_4 with C_2+ (generally C_2H_6 and/or C_3H_8) as surrogates of natural gas. Dagaut et al. [15] investigated the impact of H_2 enrichment upon the oxidation kinetics of a CH_4/C_2H_6 (10:1) mixture in a jet-stirred reactor across lean to stoichiometric conditions, concluding that enhanced reactivity was due to the augmented production of OH radicals. Similarly, other studies [16,17]

used the spherically expanding flame configuration to investigate the impact of H_2 on natural gas, however those compositions were mainly composed of CH_4 (>95% vol.), and as such outcomes are very similar to those related to CH_4/H_2 blends. Nilsson et al. [18], employing the heat-flux (flat flame) set-up, investigated both experimentally and numerically the influence of H_2 (up to 50% addition by vol.) upon a natural gas composition of $CH_4/C_2H_6/C_3H_8$ (80/10/10 vol.%). The study similarly demonstrated an enhancement of flame speed, attributed to increases in H and OH radicals. More recently, Khan et al. [19] examined the influence of H_2 (25%, 50%, 75%, by vol.) to various multi-component natural gas compositions ($CH_4/C_2H_6/C_3H_8$). It was concluded that H_2 addition lowered Le, with flames containing the highest concentrations of CH_4 most affected.

Clearly, the experimental study on the addition of H_2 on natural gas blends containing varying quantities of C_2+ is scarce, hence the aim of this work was to investigate in-detail the influence of changing Le on-flame behaviour, in the context of plausible short-term variation in multi-component natural gas blends. CH_4/C_3H_8 and CH_4/H_2 blend ratios were varied across a limited range, representative of the prospective demands of fuel-flexible natural gas combustors widely employed for power generation. The use of Liquefied Natural Gas (LNG) can lead to higher hydrocarbons in the fuel mixture [15] with C_3H_8 chosen as a surrogate in this study. It is hypothesised that the effect of this higher hydrocarbon fuel contrasts with the potential introduction of H_2 to the gas grid, as proposed in the power-to-X concept. Addition of either H_2 or C_3H_8 to a given CH_4/air mixture increases flame temperature, reactivity, and mixture flame speed and induces a change in extinction response. The change in diffusive behaviour for each of the aforementioned mixtures was studied in a fundamental laminar flame configuration, with the knowledge gained then extended to studies of tertiary blends ($CH_4/C_3H_8/H_2$) containing varying molar content of CH_4/C_3H_8 at a fixed H_2 content (15% by vol.).

2.Experimental Facilities

Laminar flame speed measurements were performed using a constant-volume cylindrical bomb (CVCB). Details of the rig and post-processing technique can be found in [20,21], and thus only a brief summary is presented here. A schematic overview of the experimental facility is presented in Fig. 1. The cylindrical CVCB (Fig. 1[a]) has a nominal internal volume of 34 L (260 mm ID), with four orthogonal 100 mm quartz viewing windows (Fig. 1[b]) with PID temperature control (Fig. 1[c]). High-speed Schlieren imaging of flame propagation was achieved using a CCD highspeed camera (Fig. 1[d] – Photron FASTCAM APX-RS (±0.05%)) set to capture 5,000 fps and facilitating a spatial resolution of ~0.14 mm per pixel. Flame propagation rates were calculated by edge-detection algorithms written into a bespoke MATLAB script. Reactants were introduced into the chamber using batched mass-flow control (Fig. 1[e] – Bronkhorst mini-CORI-FLOW devices (±0.5%)). Mass fractions were calculated as a function of initial pressure (P), fuel-air equivalence ratio (Φ), and temperature (T), with mixture concentrations confirmed by partial pressure (Fig. 1[f] – Edwards ASG 0–0.2 MPa transducer (±0.2%), resolution 1×10^{-5} MPa). A diaphragm pump (Fig. 1[g]) was used to evacuate the CVCB three times between tests to reduce errors arising from imperfect vacuum (< 1%), with the remaining air compensated in the equivalence ratio calculation. Internal fans were used to pre-mix the reactants, and capacitor-discharge ignition was achieved via fine electrodes mounted at 45° to the measurement plane. Experiments were triggered by a simultaneous TTL signal to the ignition and data acquisition systems after quiescence had been attained.

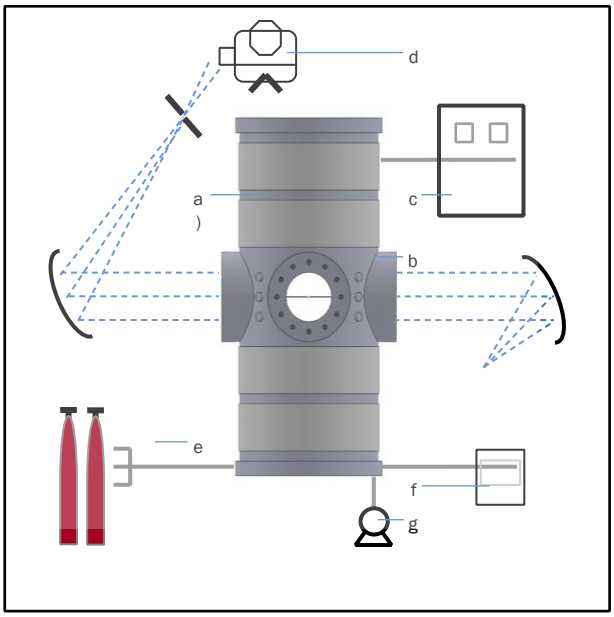

Fig. 1 – CVCB schematic (components described in text)

3.Experimental Specifications and Theory

High-purity fuel components of CH_4 (>99.995%), H_2 (>99.999%), C_3H_8 (>99.95%) and dry zero-grade compressed air were metered using the aforementioned mass-flow controllers. Measurements were performed at initial conditions of 298 K (± 3 K) and 0.1 MPa (± $1x10^{-3}$ MPa). To investigate the influence of elevated Le, a molar C_3H_8/CH_4 ratio of 15:85 was studied for a range of lean equivalence ratios (Φ = 0.60 – 1.0), representative of concentrations of higher hydrocarbons found in natural gas [1,2,15]. At a fixed equivalence ratio of Φ=0.65, the molar C_3H_8/CH_4 ratio was subsequently varied from 0-100%, to quantify the sensitivity of the lean flame response. Similarly, to investigate the influence of a decreasing Le, a H_2/CH_4 mixture also fixed at 15:85 was studied across a range of equivalence ratios (Φ = 0.60 – 1.0), and at a fixed equivalence ratio of 0.65 (with H_2 content incrementally increased; 0 – 50% by vol.%) to provide a comparison of the change in flame speed and stretch-related behaviour with each of the blends. Finally, a preliminary study of the impact of tertiary blends was undertaken; five hydrogen-enriched natural gas blends were investigated, at fuel lean conditions (Φ = 0.60 – 8.0) with compositions presented in Table 1.

Table 1 – Composition of Selected Natural Gas Blends

Fuel Designation	Fuel Composition (Volume %)		
	CH_4	C_3H_8	H_2
NG 1	68	17	15
NG 2	73.1	11.9	15
NG 3	76.5	8.5	15
NG 4	78.2	6.8	15
NG 5	79.9	5.1	15

Schlieren measurements were undertaken using an established technique and in a similar way to many contemporary studies [2,22,23] with the shadowed edge taken to indicate the burned gas isotherm, critical for characterising the influence of flame stretch as discussed by Giannakopoulos et al. [24]. Scaled images determined the Schlieren spherical radius (r_{sch}), with limits used to minimise spark and pressure effects. Bradley et al. [25] suggest a spark affected radius up to 6 mm for CH_4/air flames; however this radius has been shown to be dependent on Le [26]. In this study 10 mm was chosen as the minimum radius employed, with preliminary investigations demonstrating minimal variation in results derived from data above 8mm (ignition energy ranged between 55–170 mJ). To limit pressure effects a maximum usable radius of 35 mm was utilised, within the 30% of chamber radius as originally proposed by Burke et al. [27], and satisfying $r_{sch}/(3V/4\pi)^{1/3} < 25\%$ as suggested in the detailed analysis by Chen [28]. Extrapolation methods utilised to yield flame speed and corresponding L_b rely on a sufficiently large stable non-cellular flame regime. Therefore, due to known instability issues associated with lean combustion of H_2-containing fuels, minor modifications in usable flame radius selection were required. H_2 flames are particularly unstable with regard to diffusive effects, due to the low Le (Le<<1), with cellularity developing at early stages of flame propagation. This results in flame acceleration at decreased stretch rates [29]. As demonstrated by Gu et al. [30], flame acceleration related to cellular instabilities occurs at a critical radius to flame thickness ratio, defined by the Peclet number. Here, the critical radius was determined to be ~ 25mm for CH_4/H_2 (50/50 vol%). Hence, a conservative flame limit of ~ 22 mm was adopted for all CH_4/H_2 blends, although this critical radius was shown to increase with decreasing H_2 fraction. It is noted that for CH_4/H_2 flames containing < 25 vol% H_2, no discernible signs of flame self-acceleration were observed, with average relative differences between the initial and reduced flame radius data range (i.e., 10-35 and 10-22 mm) less than 3% and 15% for flame speed and L_b, respectively. These differences are in good agreement with previous studies which investigated the influence of flame radius range selection upon flame propagation and L_b [28,31]. Nevertheless, using a suitably fast frame capture rate, a minimum of 60 data points were obtained for even the fastest flames, from which flame speed data were derived.

For an outwardly propagating spherical flame, the stretched flame speed (S_n) is expressed as the temporal (t) derivative of the Schlieren flame radius (r_{sch}) as given in Eqn. (1).

$$S_n \frac{dr_{sch}}{dt} \qquad \text{Eqn. (1)}$$

The flame stretch rate (α), defined as the change in area (A) gradient as the flame stretches with growth, is calculated for a propagating spherical flame as shown in Eqn. (2):

$$\alpha = \frac{1}{A} \cdot \frac{dA}{dt} = \frac{2}{r_{sch}} \cdot \frac{dr_{sch}}{dt} \qquad \text{Eqn. (2)}$$

The stretch rate defined for this method of flame speed measurement encompasses both the influence of flame curvature (α_c) and flow-field strain (α_s), $\alpha = \alpha_c + \alpha_s$ as demonstrated by Bradley et al. [25]. Various correlations between S_n and α have been previously proposed, enabling unstretched flame speed (S_u), to be attained through extrapolation of S_n to zero stretch rate, with both S_u and L_b determined from the measured results with respect to the burned gas. Wu & Law [32], proposed a linear relationship, based upon the assumption that mass and thermal diffusion are near equal (Le≈1) and that the flame is weakly stretched. Taylor [33] and Dowdy et al. [34], employing this reasoning, suggest that α and flame speed are related in the following manner Eqn. (3):

$$S_u - S_n = L_b \cdot \alpha \qquad \text{Eqn. (3)}$$

It may be noted that L_b characterises the effect of stretch on flame propagation, with the sign and magnitude of L_b directly related to Le. S_u is subsequently derived by extrapolation of the relationship to a corresponding intercept value (α=0), equivalent to a theoretical spherical flame of infinite radius. Here, this methodology will be referenced as LM(S) (i.e., Linear Model based on flame stretch).

The second methodology, is a model attributed to Frankel and Sivashinksy [35], originally proposed by Markstein [36], based upon the assumption of large flame radii. Frankel and Sivashinksy analysed a spherically expanding C_3H_8 flame, considering the effects of thermal expansion and Le, obtaining the following relationship in Eqn. (4):

$$S_n = S_u - S_u \cdot L_b \cdot \frac{2}{r_f} \qquad \text{Eqn. (4)}$$

Eqn. (4) shows that the flame curvature ($\kappa = 2/r_f$) and S_n vary linearly. As such, S_u and L_b can be obtained from linear extrapolation, of S_u and κ [37,38]. This methodology has not received widespread use [21,39] and here is referenced as LM(C) (i.e. Linear Model based on Curvature).

Kelley and Law [40] proposed a non-linear model, based upon the theoretical work of Ronney and Sivashinsky [41]. This extrapolation technique allows for arbitrary Le and accounts for deviations in adiabatic and planar assumptions, which are more prominent for flames heavily influenced by stretch [34], such as lean H_2 or C_3H_8 flames. This non-linear relationship is expressed in Eqn. (5):

$$\left(\frac{S_n}{S_u}\right) \cdot In\left(\frac{S_n}{S_u}\right)^2 = -\frac{2 \cdot L_b \cdot \alpha}{S_u} \qquad \text{Eqn. (5)}$$

A quasi-steady nonlinear association between S_n and α is employed -rearranged with the error used for least squares regression- to obtain an extrapolated unstretched flame speed. This methodology has been used frequently over the last decade, improving accuracy [31,38]. Here this method will be referred to as NM(S) (i.e., Non-Linear Model based on Stretch).

The uncertainty in extrapolation was investigated by Chen [37] and Wu et al. [38], concluding that the accuracy of the different extrapolation techniques depend strongly upon Le of the fuel air mixture. Chen demonstrated that LM(S) is suitable for mixtures with Le close to unity, whilst LM(C) and NM(S) are to be preferred for mixtures with Le>1 (positive L_b) & Le<1 (negative L_b), respectively, because of the nonlinear trend in relationship of S_n and α. These recommendations have been adopted in this work.

Irrespective of the extrapolation methodology employed, burned gas expansion must be accounted for to obtain representative values of laminar flame speed (U_L). This adiabatic expansion at constant pressure, can be termed as the ratio of the burnt (ρ_b) and unburnt (ρ_u) gas densities. U_L can thus be evaluated through, $U_L = S_u \cdot (\rho_b/\rho_u)$, with adiabatic densities calculated using CHEMKIN-Pro, employing the Aramco 1.3 chemical reaction mechanism [42], as discussed further in section 5.2.

4.1. Evaluation of Fundamental Flame Parameters

Theoretical relationships linking L_b to Le have been proposed previously, notably by Chen [26,37] and Matalon and Bechtold [43]. These theoretical correlations require the calculations of various fundamental flame parameters. The Zel'dovich number, was evaluated using the expression $Ze = E_a(T_{ad} - T_u)/(R^0 T_{ad}{}^2)$, with R^0 the universal gas constant, T_u and T_{ad}, the temperature of the unburnt mixture and the adiabatic flame temperature, respectively. The activation energy, E_a, is defined as the slope of the mass burning flux (m^0) and the inverse adiabatic flame temperature at constant Φ and pressure, empirically determined using the expression $E_a = -2 \cdot R_u \cdot \partial$

$[ln(m^0)]/\partial[1/T_{ad}]$, where the mass burning flux is the eigenvalue of laminar flame propagation, and can be replaced by $m^0 = (\rho_u \cdot U_L)$, as recommended by Egolfopoulos and Law [44]. Two methods are commonly employed to vary the mass burning flux, required to evaluate the differential, the first by slightly perturbing the diluent concentration [44,45]. However, Kumar and Sung [46] note that by varying m^0 and T_{ad} through different levels of N_2 dilution, the reactant concentrations are also altered. As such, the second method, based upon preheating the unburnt gas, is advised. Consistent with previous studies [46,47], the second method was applied here, achieved by varying the unburnt gas temperature in CHEMKIN-Pro PREMIX. The linear variation of $ln(m^0)$ and $(1/T_{ad})$ observed during this work validates this extraction method, with R-Squared values (R^2) of at least 0.999. Note, however, that this method is only valid for sufficiently off-stoichiometric conditions, with E_a values for mixtures near stoichiometry requiring interpolation [41].

Two definitions of the laminar flame thickness have been previously proposed and deployed [7]. The first, commonly referred to as the kinetic (diffusion) thickness (δ_K), is given by $\delta_K = \lambda/(\rho_u \cdot c_p \cdot U_L)$, where ($\lambda$) represents the thermal conductivity, and (c_p) the specific heat. Jomaas et al. [48] underline the ambiguity of this definition, most notably at which temperature the ratio (λ/c_p) should be assessed. As such, an expression of the flame thickness relying upon the extraction of the gradient temperature profile with axial distance through the flame is proposed [7,48]. This approximation relies upon the application of a linear gradient as the tangent of the inflection, which corresponds to $(dT/dx)_{max}$, which was numerically modelled using the CHEMKIN-Pro software. This flame thickness, referred to as the gradient thickness (δ_G), can be expressed as $\delta_G = (T_{ad} - T_u)/(dT/dx)_{max}$. The kinetic flame thickness definition is consistent with the approach detailed by Chen [26,27], whilst the gradient flame thickness definition is consistent with the approach detailed by Bechtold and Matalon [43], and thus each are employed accordingly in the derivations of Le and L_b as defined by the given authors. Finally, for the sake of completeness, the thermal expansion ratio ($\sigma = \rho_u/\rho_b$) applied is consistent with the approach described by Matalon [43].

4.2 Relationships of Le and L_b

In this work, two theoretical relationships linking L_b to Le have been utilized, as proposed by Chen [26,37] and Matalon and Bechtold [43]. The first method is derived from the analytical developments conducted by Chen on spherically expanding flames, since employed by Lapalme et al. [39] and Bouvet et al. [49] in their studies concerning Le effects for multi-component fuels. This method is denoted here as Le_{CHEN}, and is expressed per Eqn. (6):

$$Le_{CHEN} = \left[\frac{L_b}{\sigma \cdot \delta} - \frac{Ze}{2}\right]^{-1}\left[1 - \frac{Ze}{2}\right] \quad \text{Eqn. (6)}$$

From Eqn. (6) the retrieval of L_b is possible as shown in Eqn. (7).

$$L_{b-CHEN} = \left[\frac{1}{Le} - \left(\frac{Ze}{2}\right)\left(\frac{1}{Le} - 1\right)\right]\sigma \cdot \delta \quad \text{Eqn. (7)}$$

A second formulation by Bechtold and Matalon [43], derived from their theoretical research on the dependence of L_b on stoichiometry, was demonstrated valid for off-stoichiometric conditions. This formulation has been employed by Jomaas et al. [48], for the determination of Le of acetylene (C_2H_2) in air across a wide range of conditions, and employed by Lapalme et al. [39] for H_2/CO and H_2/CH_4 mixtures. This relationship is denoted herein as Le_{BM}, and is expressed per Eqn. (8):

$$Le_{BM} = 1 + \left[\frac{L_b}{\delta} - \frac{2}{\sqrt{\sigma}+1}\right]\left[\frac{2 \cdot Ze}{\sigma - 1}\left\{\sqrt{\sigma} - 1 - In\left(\frac{1}{2}\left(\sqrt{\sigma}+1\right)\right)\right\}\right]^{-1} \quad \text{Eqn. (8)}$$

Eqn. (8) can be re-arranged to retrieve L_b, and is defined as $L_{b\text{-}BM}$ as per Eqn. (9):

$$L_{b-BM} = \delta\left[\frac{\gamma_1}{\sigma} - \left\{\frac{Ze}{2}(Le - 1)\gamma_2\right\}\right] \quad \text{Eqn. (9)}$$

where γ_1 and γ_2 are functions of the expansion ratio given in Eqn. (10) and Eqn. (11):

$$\gamma_1 = \frac{2 \cdot \sigma}{\left(\sqrt{\sigma}+1\right)} \quad \text{Eqn. (10)}$$

$$\gamma_2 = \left[\frac{4}{\sigma - 1}\right]\left[\sqrt{\sigma} - 1 - In\left(\frac{\sqrt{\sigma}+1}{2}\right)\right] \quad \text{Eqn. (11)}$$

4.3 Lewis Number evaluation of multi-component mixtures

For multi-fuel blends, the calculation of Le can become challenging since the diffusivity of each fuel must be considered. This is especially applicable to blends of H_2 and hydrocarbons, which exhibit different transport diffusion mechanisms and flame characteristics. Whilst the calculation of Le for single-fuel mixtures can be considered relatively straightforward, there is little consensus on the correct formulation of Le to be employed for multi-fuel blends [49]. Bouvet et al. [49] identified three 'effective' Le formulations (Le_{eff}). The first derived by Law et al. [23] was from the asymptotic analysis of high pressure H_2/C_3H_8 laminar spherical flames. This formulation has been extensively applied to discuss the thermo-diffusive behaviour (i.e. stable, Le>1 or unstable Le<1) of mostly binary and tertiary blends of hydrocarbons and hydrogen [14,50–52]. Based upon the weighted average of the fuels' nondimensional heat release (q_i), a heat release weighted formulation, referenced in this work as Le_H, can be expressed as Eqn. (12a):

$$Le_H = 1 + \frac{\sum_{i=1}^{f} q_i(Le_i - 1)}{\sum_{i=1}^{f} q_i} \quad \text{Eqn. (12a)}$$

where

$$q_i = \frac{Q \cdot Y_{i,unburnt}}{c_p \cdot T_u} \quad \text{Eqn. (12b)}$$

And (Q) represents the overall heat of reaction, Y_i, the mass fraction of species 'i'.

The second Le formulation is based upon a volumetric fraction weighted average, stemming from the computational study of turbulent $CH_4 – H_2/C_3H_8$ flames by Muppala et al. [8]. This formulation led to reasonable agreement with experimental burning velocities at low turbulence intensity. However, it is noted that differences between measured and modelled flame speeds increased at higher turbulent intensity, with modelled burning rates significantly underpredicting measurements. This, volume weighted, formulation will be referenced in this work as Le_V, and is expressed per Eqn. (13):

$$Le_V = \sum_{i=1}^{f} x_i \cdot Le_i \qquad \text{Eqn. (13)}$$

where (x_i), is the fuel volumetric fraction of the component 'i'.

Finally, Dinkelacker et al. [14] using lean H_2/CH_4 flames assumed that if flame curvature is dominant, then local enrichment of the most diffusive fuel at the flames leading edge can be expected. This overall reaction-rate enhancement is translated into a volumetric-weighted average of the fuel diffusivities. This, diffusion weighted, formulation will be referenced in this work as Le_D, and is expressed per Eqn. (14):

$$Le_D = \frac{D_T}{\sum_{I=1}^{F} x_i \cdot D_{ij}} \qquad \text{Eqn. (14)}$$

where D_T is the mixture's thermal diffusivity and D_{ij} are the binary mass diffusion coefficients. Several methods have been proposed to estimate the binary mass diffusion coefficients of moderate pressure gases (<10 bar), with empirical constants based upon experimental data [53]. The proposals of Hirschfelder, Bird and Spot, as well as that of Wilke detailed in [53], have been employed in this study. Once the binary coefficients for the combinations of gases are estimated, an effective formulation of the deficient species in the mixture must be selected. Conventionally, it is assumed that for lean fuel-air mixtures, the deficient reactant is scarce compared to the surrounding N_2 [7]. Consequently, D_{ij} is taken as the fuel '*i*' diffusing into N_2 (denoted with the subscript 'j'). Thus, the binary coefficients are evaluated employing the assumption that the fuel is diffusing into N_2. As highlighted by Lapalme [39], this may hold true for hydrocarbons due to their high molar fuel-air ratio, but not for fuels that have low molar fuel-air ratio such as H_2. Thus, the mixture-averaged coefficient of mass diffusion into the mixture as proposed by Wilke [54] was selected here, with details of the method available in [21]. The binary diffusion coefficients attained in this study exhibit good agreement with values evaluated using the STANJAN transport calculator [55], with differences no greater than $\pm$2% for the various binary compositions composed of hydrocarbons, O_2 & N_2 and up to 10% in the presence of H_2, which is in line with expected deviation [53]; hence the derived coefficients are considered suitable for the purpose of this work.

5. Results and Discussion

5.1 Pure Fuels

Prior to discussing results, it should be stressed that L_b is indicative of the influence of stretch on flame speed. In premixed flames, instabilities result from both hydrodynamic (Darrieus-Landeau) and preferential-diffusional (Le) instabilities [7,30]. Hence, in this study, experimental or theoretical L_b are utilised as a measure of a flame's susceptibility to instability and should only be viewed as indicative of the effect, not the cause. Historically, the combustion characteristics of CH_4 have been studied extensively using the spherically expanding flame configuration [30,31,33,56–58], however it should be noted that there remains relatively large scatter in the derived U_L and corresponding L_b values (see Supplementary Material S.1 & S.2). Large discrepancies that exist, up to 100% for L_b, have been attributed to mixture preparation (accuracy of Φ) as well as the correct selection of a suitable extrapolation technique for the fuel investigated, with stretch-models strongly dependent upon the Le of the mixture [37]. Furthermore, slope inversion of L_b (from positive to negative) for CH_4 (Φ < 0.60) has been reported several times [33,56,58] with opposed L_b consistently reported too [30,31], see S.2. A quantitative explanation behind these divergences has yet to be proposed, with behaviour either attributable to a physical-chemical phenomenon or uncertainty generated when extrapolating data. Published evaluations of the Lean Le Limit for CH_4 flames, range between Le = 0.955 [14] and 1.01

[39], marginally above and below the critical value (Le = 1). Consequently, two opposite flame behaviours are predicted for the same limit, with both measured experimentally (positive and negative L_b). From a simple mass diffusion perspective (CH_4, N_2, O_2 in this case), the relative diffusivities of the reactants relative to N_2 gives CH_4 is greater than O_2. For ultra-lean CH_4/air mixtures, increased stretch would increase local CH_4 concentration within the flame front, thereby increasing burning intensity (through augmented flame temperature), influencing flame behaviour [59].

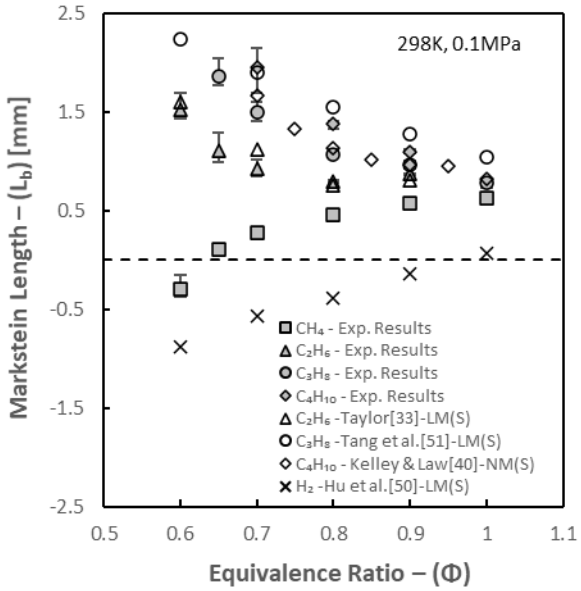

Fig. 2 – Experimental L_b for CH_4, C_2H_6, C_3H_8, C_4H_{10} H_2 comparison across lean Φ

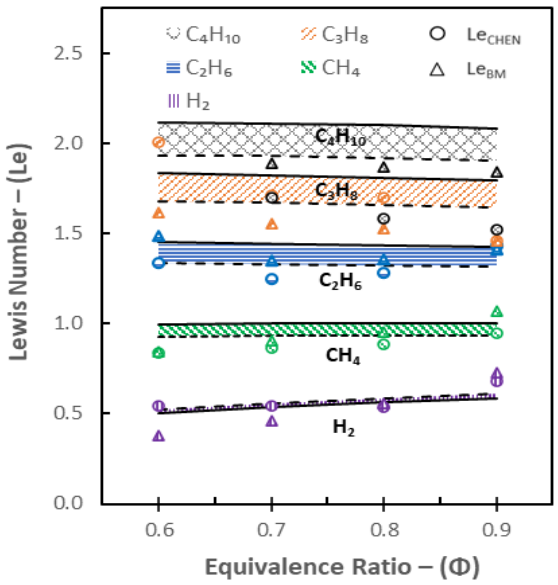

Fig.3 – Theoretical and Experimental Le for and lean CH_4, C_3H_8 and H_2 (H_2 Exp. data [50]) Full & dotted lines reflect Hirschfelder & Wilke methods to evaluate D_{ij} (298K, 0.1MPa)

Fig. 2 illustrates measured L_b for the primary components of natural gas (C_1-C_4) and H_2 under lean conditions. Note that all datasets presented in Fig. 2 were conducted at similar temperature (±5K) and pressure conditions, to those employed in this work. To facilitate fair comparison, the relationship relating flame speed to stretch employed to extrapolate L_b is also referenced. Flame characteristics of higher hydrocarbons (C_2H_6, C_3H_8, C_4H_{10}) have been studied less than CH_4, although it is noted that there is a substantial literature of flame speed measurements for C_2H_6 [1,33,60], C_3H_8 [1,33,60] and C_4H_{10} [1,40], though considerably less so for measured L_b. Konnov et al. [61] recently undertook an exhaustive compilation of measured flame speeds for C_2+/air flames generated using various experimental set-ups. The study highlights the scarcity of unstretched flame speed data for C_2H_6 and C_3H_8, particularly in the case of spherically expanding flame configuration data, derived using contemporary nonlinear extrapolation techniques. Data illustrated in Fig. 2 fulfils this gap in knowledge under lean conditions, with corresponding U_L values provided in S.3. To highlight the influence of the extrapolation model on L_b values, average relative differences in measured L_b values for lean $C_{1\text{-}4}$/air mixtures, using LM(S) and NM(S) normalised to LM(C), are illustrated in S.4. Clearly, for fuels exhibiting Le >>1 (i.e. $C_{2\text{-}4}$), LM(S) overpredicts L_b values, with differences augmenting with increasing hydrocarbon number and decreasing Φ (reflecting an increasing Le), with significantly reduced differences recorded in relation to NM(S), in good agreement with the theoretical analysis conducted by Chen [37]. The same general trend is upheld when analysing unstretched flame speed, however, differences are substantially smaller (<10%), irrespective of the extrapolation model employed.

As can be seen in Fig. 2, at stoichiometric conditions, similar stretch-related behaviour (positive L_b) are measured for C_{1-4} alkanes and H_2 (H_2 data sourced from Hu et al. [50], with positive L_b at Φ=1.0 also reported by [29,51]). With respect to the C_{1-4} fuels studied, increased variations in L_b occur as conditions shift leaner, with CH_4 and C_2-C_4 exhibiting opposing trends. It is noted that CH_4 displays a behaviour characteristic to that of H_2, with L_b decreasing at leaner conditions.

Fig. 3 presents the Le behaviour of H_2 and C_{1-4} alkanes under lean conditions. 'Theoretical' Lewis numbers, evaluated using the free stream properties of the mixtures, are illustrated as coloured bands, with the upper and lower limits (represented by full and broken lines) denoting the differences resulting from the application of either the Hirschfelder or Wilke method of mass-diffusion coefficient evaluation. Although the correct Le is evaluated (Le~1, Le>1, Le<1, for CH_4, C_{2-4}, H_2 respectively), little variation is observable across the Φ range tested. Fundamental flame parameters such as the activation energy, flame thickness and thermal expansion, have been demonstrated to vary significantly for off-stoichiometric mixtures [43], influencing the flame's sensitivity to stretch. Variations in those fundamental characteristics are not considered, since Le is evaluated simply as a function of the mixture's thermal and mass diffusivity. As such, Le was evaluated from properties affecting the flame, attained experimentally (via L_b) and numerically (via E_a, σ, δ), rendering Le a global parameter of the flame, as recommended by Jomaas et al. [48], through the use of theoretical relationships proposed in literature (denoted as Le_{CHEN} & Le_{BM}). Evidently, as can be seen when comparing Fig. 2 and Fig. 3, analogous L_b and Le behaviour is apparent, irrespective of the theoretical relationship linking L_b to Le. Increasingly contrasting Le behaviour, with decreasing Φ, is observable for CH_4 and C_{2-4} alkanes (less so for C_2), consistent with their measured stretch-related behaviour. It should be noted that for H_2, whilst exhibiting a positive measured L_b at stoichiometric conditions, all experimental Le formulations result in Le < 1.

The lean and rich limits of Le for each fuel (CH_4, H_2, C_{2-4}) were evaluated to assess how well the considered formulations captured Le behaviour. The Le limits bound the minimum (lean) and maximum (rich) plausible Le values for ultra-lean and ultra-rich mixtures. Note that lean limits are largely dictated by mass-diffusion of fuel into N_2 (Φ < 1), with rich limits dictated by mass diffusion of O_2 into the fuel (Φ > 1). Although no experiments under rich conditions were conducted in this study, evaluations of the rich limit allow understanding of plausible variation of Le with changing Φ. To evaluate these limits, the upper and lower flammability limits of the fuels were utilised. For CH_4, lean and rich limits were calculated to be 0.93 and 1.06, respectively, marginally smaller than those reported previously, namely 0.955 [14] and 0.98 [62] on the lean side, and 1.10 [39] on the rich side, underlining its equi-diffusive nature. Clearly, it can be seen from Fig. 3 that Le_{CHEN} better respects these limits, particularly at richer conditions, with Le_{BM} marginally above the rich limits at Φ = 0.9, with the rising Le trends expected to increase further at richer conditions. In the case of C_2H_6, the lean limit (1.46) corresponds with Hawkes and Chen [62] value of 1.47, whilst no comparable values were found for the rich limit (0.94). It is noted that both evaluated formulations result in a similar decrease in Le between Φ=0.6-0.7, prior to a gradual increase in Le as conditions get richer, hence not satisfactorily capturing the expected decreasing Le trend as conditions get richer. With respect to C_3H_8, Le_{BM} shows closest agreement with the lean and rich limits, evaluated at 1.87 and 0.92, respectively. Again, these limits are in good agreement with those found in literature, with Law and Sung [59] citing 1.87 and 0.92, for rich and lean Le limits, respectively. With respect to C_4H_{10}, no sources were found to compare the Le limits for this fuel, with lean and rich limits slightly higher (2.04) and lower (0.88), respectively, than those of C_3H_8. However, the expected trend of decreasing Le with increasing Φ is exhibited by both formulations, most pronounced upon application of Le_{CHEN}. With respect to H_2, Le lean and rich limits were evaluated to be 0.34 and 2.02, in good agreement with literature on the lean side, 0.29 [39,62] and 0.33 [59]. The rich limit evaluated in this study (2.02) is however, smaller than other reported values, 2.32 [59] and 2.58 [39], potentially due to the underestimation of H_2 binary

mass diffusion coefficients, as highlighted previously. Overall, Le_{CHEN} best captures expected thermo-diffusive behaviour for CH_4, in agreement with Lapalme [39]. Better agreement is attained by all formulations for lean H_2 and C_{3-4} alkane combustion.

5.2 Binary Blends across Lean Φ

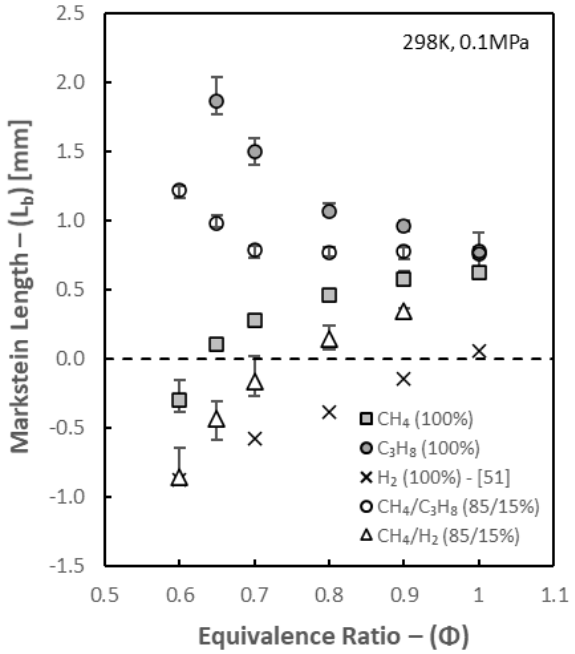

Fig. 4 – L_b vs Φ for Selected Pure & Binary Blends

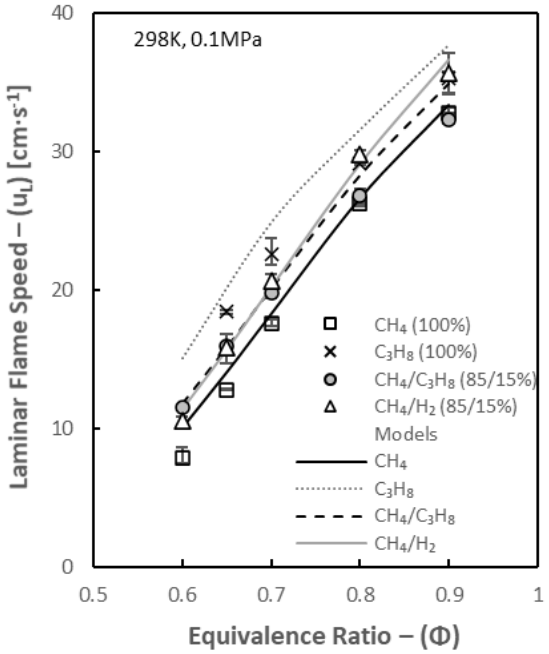

Fig. 5 – U_L for selected Pure and binary blends

Model results from Aramco 1.3

To further assess the observed opposite preferential diffusional behaviour of H_2 and C_3H_8, CH_4 was subsequently blended at 15% (vol.) with H_2 and C_3H_8 respectively, with this blend ratio maintained across Φ = 0.60 – 1.0, with Fig. 4 and 5 illustrating measured L_b and U_L values respectively. Note that unless otherwise stated, error bars represent maximum and minimum recorded values, around an average plotted value (minimum of 3 repeats), for graphs of experimental L_b and U_L values. Clearly, 15% (vol.) enrichment of CH_4 with either H_2 or C_3H_8 has limited influence on L_b approaching stoichiometry (Φ=0.90), a consequence of each specific fuels' having similar response to stretch and Le behaviour at such conditions. However, it is evident in Fig. 4 that H_2 and C_3H_8 yield increasingly divergent influence on CH_4 flame stability, with H_2 enrichment resulting in promoting preferential diffusional instabilities, reflected by measured negative L_b values. A shift in L_b sign inversion (from positive to negative) is observable, from Φ~0.60 – 0.65 for the 100% CH_4 to Φ~0.70 – 0.80 for the CH_4/H_2 blend. It should be emphasised that near equivalent stretch behaviour was exhibited by pure H_2, as measured by Hu et al. [50], and the CH_4/H_2 (85/15) mixtures at the leanest conditions. However, it is noted a linear extrapolation model [LM(S)] was utilised by Hu et al. [50], whilst a non-linear model [NM(S)] was applied in this work. As demonstrated by Chen, for mixtures exhibiting Le < 0.65, as is the case for lean (Φ<0.70) H_2 (with 'theoretical' and experimental Le < 0.60, Fig. 3), NM(S) is preferable. It thus seems probable that L_b measurements of H_2/air flames published using LM(S), greatly overpredict L_b values with H_2 displaying much lower (negative) L_b than currently reported. On the other hand, it can be seen from Fig. 4 that the CH_4/C_3H_8 (85/15) exhibits very limited change in measured L_b for Φ = 0.70 – 1.0. At leaner conditions, CH_4/C_3H_8 mixtures display a stretch response like that of pure C_3H_8, with a transition point apparent at Φ~0.70; this characteristic is investigated further in Section 5.3.

Fig. 5 presents the measured U_L values of selected pure fuels tested binary blends alongside values attained numerically. USC-II (2007) [63], GRI-Mech 3.0 (1999) [64], San Diego (2014) [65] and Aramco 1.3 (2013) [42] reaction mechanisms were all appraised, however only the latter is illustrated since it consistently gave best agreement with all blends evaluated in this study. As can be seen from Fig. 5, the addition of either H_2 or C_3H_8 to ultra-lean (≤ 0.70 Φ) CH_4-based flames resulted in significant relative increases in flame speed (at Φ=0.60 relative increase in S_u ~30% and ~37% upon 15% vol. H_2 or C_3H_8 addition, respectively), with augmentation in flame propagation substantially decreasing at increasingly richer conditions, with C_3H_8 addition resulting in nominal U_L enhancement at Φ>0.80. The CHEMKIN-Pro package employing the PREMIX module, to simulate a premixed 1-D adiabatic planar flame, was used to provide better understand reactivity trends displayed in Fig. 5. A simulation domain of 10 cm was considered, with a total of 1000 grid points used with grid parameters GRID (0.025) and CURV (0.1), including multi-component diffusion and an assumed air composition of 79% N_2 – 21% O_2. The Aramco 1.3 reaction mechanism was utilised to generate numerical volumetric heat release rates (Q') and concentration of mole fractions of active radicals (H and O). Relative changes in measured S_u and numerically attained Q', H and O mole fractions, normalised to that of pure CH_4, across lean conditions (Φ=0.6 – 0.9), are presented in Figure 6.

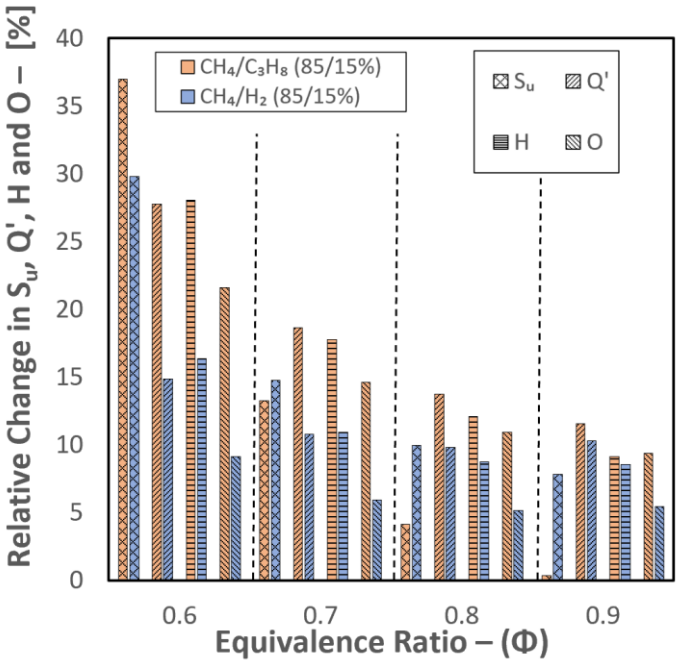

Fig. 6 – Relative changes in measured S_u and modelled Q', H and O mole fraction concentration, normalised to that of pure CH_4, for CH_4/H_2 and CH_4/C_3H_8 (85/15% vol.) blends at Φ = 0.6 – 0.9.

Interestingly, volumetric additions of 15% C_3H_8 or H_2 to ultra-lean CH_4 flames (≤ 0.70 Φ) produce comparable flame propagation effects. The increased reactivity of lean CH_4/H_2 flames has been suitably reported [21,66], with modelling work and sensitivity analysis suggesting that the flame speed, burning intensity (Q'), and production of radicals (notably H), appear to be strongly correlated, in agreement with measured and modelled values presented in Fig. 6. Furthermore, as evident from Fig. 6, at near stoichiometric conditions (Φ = 0.9), C_3H_8 (15%) addition to CH_4 results in practically similar relative increase in Q' as H_2 addition (15%). However, when moving towards leaner conditions, C_3H_8 additions yield higher relative increases in Q' than H_2 addition, practically double at leanest conditions (Φ=0.60), in agreement with witnessed S_u augmentations. It should be emphasised that the heat of combustion per mass (kJ/mol) of H_2 is 2 to 3 times greater than that of C_3H_8, however there are significant differences in terms of molecular mass between both fuels consequently suppressing the higher heat of combustion exhibited by H_2. Comparison of relative increases in

production of radical fractions (H and O) in CH_4 flames due to the addition of H_2 or C_3H_8 (15% vol.) are plotted in Fig. 6. Modelled values predict an enhanced production of radicals related to the presence of C_3H_8 than H_2, with differences in radical production increasing with decreasing Φ, highlighting the importance of small amounts of hydrocarbons on the oxidation mechanics of CH_4. When no other fuel is present, CH_4 oxidation is initiated by its reaction with O_2 and by thermal dissociation [7,67]. For the lean CH_4/C_3H_8 blends, C_3H_8 reacts first, leading to the formation of radicals enhancing the oxidation mechanics of CH_4, leading to similar increases in both burning intensity and reactivity, reflected by augmented flame speeds. Thus, both H_2 and C_3H_8 promote flame propagation of ultra-lean methane-based fuels, to a similar extent for 15% volumetric enrichment levels, however, yield opposite stretch related and Le behaviour.

5.3 Experimental and Numerical Study of Binary Blends

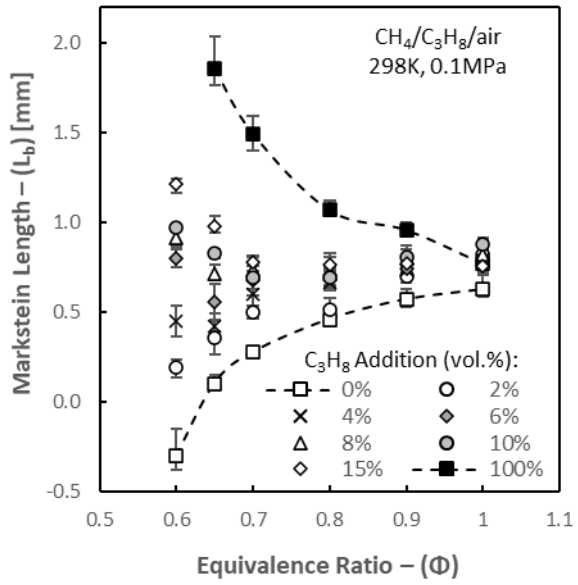

Fig. 7 – L_b vs Φ for CH_4/C_3H_8

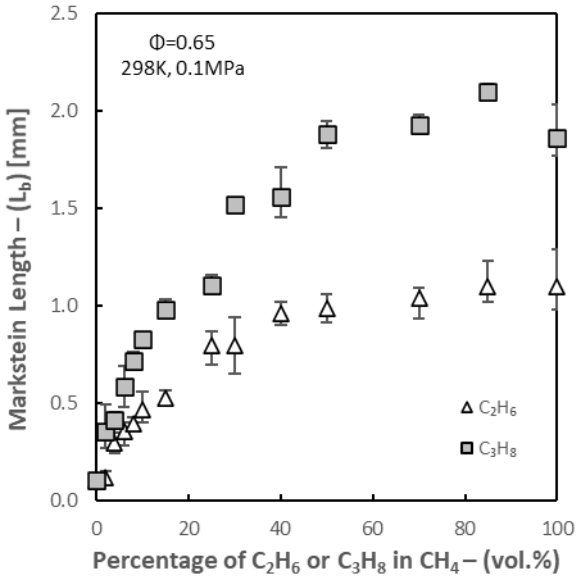

Fig. 8 – Influence of Fuel Mixtures on L_b

To investigate the thermo-diffusive influence of small additions of C_3H_8 on CH_4, practically representative of natural gas variations, a study was conducted under lean combustion conditions (Φ=0.60 – 1.0). L_b behaviour is illustrated in Fig. 7. with all CH_4/C_3H_8 blends exhibiting similar stretch-related behaviour at Φ ≥ 0.70, with minimal variation in measured L_b. At leaner conditions, the C_3H_8 component becomes noticeable, with blends containing up to 4% C_3H_8, maintaining a L_b behaviour reflective of that of CH_4, where L_b decreases at increasingly leaner conditions. This alludes to the fact that mass diffusion becomes increasingly more prevalent, whilst still not becoming the dominant transport mechanism. Blends containing greater than 6% C_3H_8, start displaying a noticeable rise in measured L_b, notwithstanding that the mixtures are still predominantly CH_4 (molecular weight ratio ~5.5:1 for a 94/6% CH_4/C_3H_8 blend), with relatively small concentrations of C_3H_8 dictating the flames response to stretch. To investigate the influence of heavier hydrocarbons on stretch response of lean CH_4 based fuels further, a study of CH_4/C_2H_6 and CH_4/C_3H_8 blends at a fixed Φ = 0.65 was undertaken, with L_b measurements illustrated in Fig. 8. Clearly, relatively small additions of heavier hydrocarbons (<15%) yield a significant response on the stretch-sensitivity of CH_4, naturally with this effect increasing the heavier the hydrocarbon, as a direct consequence of the blends increasing Le. With respect to C_2H_6 addition, it is noted that there appears to be two distinctive trends, with important incremental changes in L_b response up to 25% additions, prior to an observed plateauing in L_b, arising when the molecular weight ratio of the CH_4/C_2H_6 blend is near equal (~1:1, 65/35%). Little change in stretch response is reported beyond this point, with behaviour akin of pure C_2H_6 exhibited upon any

further enrichment. A similar response is noted with the CH_4/C_3H_8 blends, with important incremental increases in L_b up to 30% C_3H_8 content, although a more linear response is observable compared with the CH_4/C_2H_6 blend.

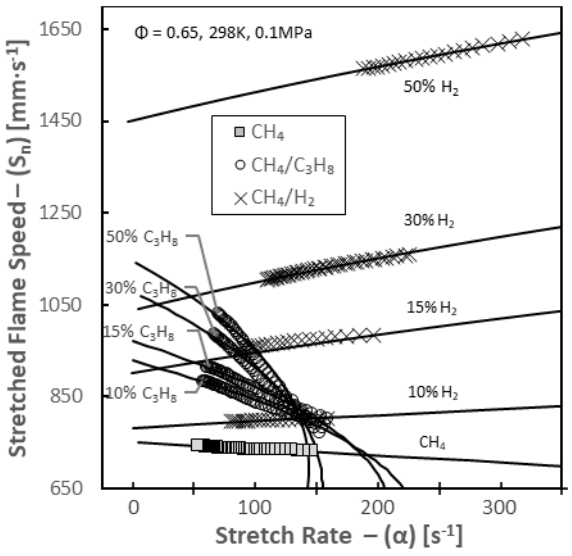

Fig. 9 – Stretch Response of CH_4 with H_2 and C_3H_8

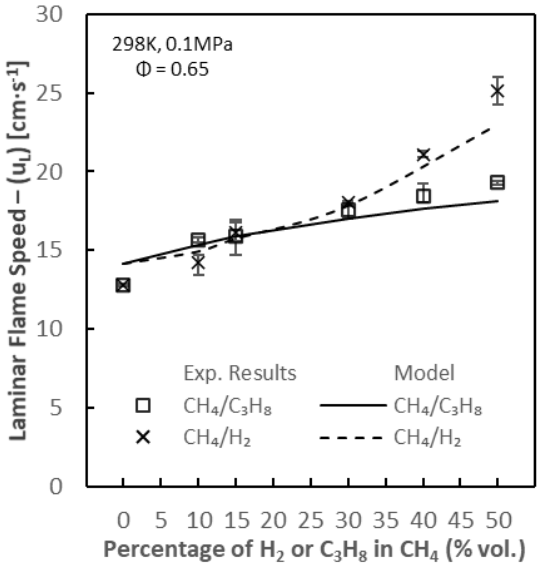

Fig. 10 – U_L values of CH_4/H_2 and CH_4/C_3H_8 Model results from Aramco 1.3

Fig. 9 illustrates the relationship between the stretched flame speed and stretch rate for CH_4, CH_4/C_3H_8 and CH_4/H_2 mixtures at an Φ = 0.65, with a positive gradient representative of an acceleration in flame speed with increasing stretch rates, equating to a negative L_b. Note that only one in three data points is plotted, to enhance readability, with NM(S) superimposed as solid lines. CH_4 exhibits quasi-equi-diffusion of heat and mass transport mechanisms (Le ~1), with flame propagation practically independent of stretch and curvature effects, exemplified with a gradient close to zero. Significant changes are observed with the addition of H_2, with an inversion in the gradient observable, and flames now experiencing acceleration with increasing stretch, with the opposite behaviour observed upon C_3H_8 enrichment, as shown previously in Fig. 8. Hence, a CH_4/C_3H_8 flame displaying Le > 1 (positive L_b) would be weakened in highly stretched (turbulent) environments, whilst the CH_4/H_2 exhibiting Le < 1 (negative L_b) would accelerate. This thermo-diffusive flame response inevitably impacts the operation of practical combustion systems.

Fig. 10 presents the measured laminar burning velocities of the CH_4/C_3H_8 and CH_4/H_2 mixtures for Φ = 0.65, with lines representing modelled values using the Aramco 1.3 mechanism. It is clearly observable that up to 30% enrichment of either H_2 or C_3H_8 results in similar enhancement of flame reactivity, with this trend well captured by the Aramco 1.3 mechanism. Although displaying comparable flame propagation velocities, H_2 and C_3H_8 flames exhibit opposite thermo-diffusive combustion responses with corresponding stretch-related behaviour to CH_4 based fuels. To better understand the nature of the augmented burning intensity of CH_4/H_2 and CH_4/C_3H_8 flames measured, a sensitivity analysis related to the contribution of major flame enhancing pathways (thermal, diffusive, kinetic) was undertaken. However, to correctly quantify the diffusive pathway, a suitable Le formulation must be validated.

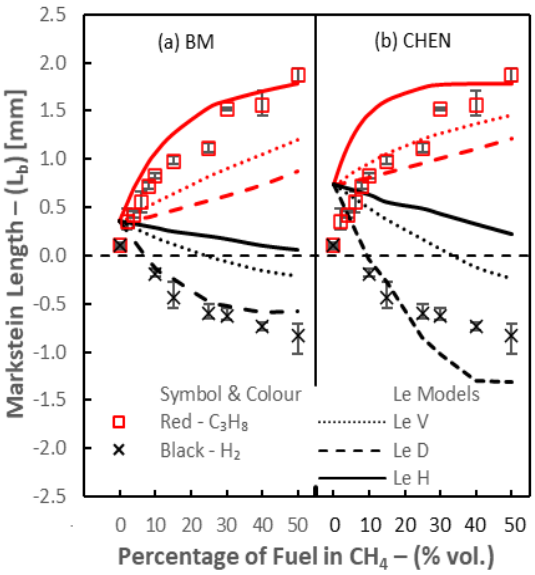

Fig. 11 – Comparison of $L_{b\text{-}BM}$ & $L_{b\text{-}CHEN}$ models to measured L_b

Consistent with methods presented earlier (Section 4.1 – 4.3), Le_{eff} models (i.e. Le_V, Le_D, Le_H) are employed in turn to yield a numerical L_b, using the relationships L_b to Le as proposed by Chen [26,37] and Matalon & Bechtold (BM) [43], referred to in text as $L_{b\text{-}CHEN}$ and $L_{b\text{-}BM}$, respectively. It should be noted that the aim of such analysis is not quantitative in nature, rather qualitative trends are sought, to validate which Le_{eff} model best captures the exhibited stretch-related behaviour of the evaluated blends. $L_{b\text{-}CHEN}$ and $L_{b\text{-}BM}$ for the CH_4/H_2 and CH_4/C_3H_8 blends are presented in Fig. 11, alongside experimentally measured L_b values. In the case of the BM formulation, both quantitative and qualitative agreement is only observed with Le_H and Le_D, for CH_4/C_3H_8 and the CH_4/H_2 blends, respectively. Minimal differences are noted between measured L_b and numerical $L_{b\text{-}BM}$ across the mixture concentrations. Furthermore, the incremental changes observed in L_b upon small enrichment fractions of C_3H_8 (2 – 15% vol.) is well captured. Poorer agreement is observed with the CHEN formulation, with again, Le_H and Le_D best reflecting expected stretch behaviour for CH_4/C_3H_8 and the CH_4/H_2 blends, respectively. The fact that an Le_D formulation displays best agreement with CH_4/H_2 at very lean conditions is expected, given that the Le_D formulation was derived from modelling of lean turbulent CH_4/H_2 flames [14]. This is influenced due to the assumption that flame curvature is dominant, hence local enrichment of the most diffusive fuel at the flames leading edge is predicted. Since for ultra-lean conditions H_2 and CH_4 have higher mass diffusivities than O_2, this concept appears valid. Bouvet et al., [49] conducted similar research, concluding that an Le_V model employing the CHEN relationship better captured changes in thermo-diffusive response of CH_4/H_2. However, Bouvet and co-workers evaluated CH_4/H_2 flame behaviour at richer conditions than presented herein, ($\Phi = 0.80$). It is noted that similar analysis was conducted at richer conditions ($\Phi = 0.80 – 1.0$) not presented herein but available in [17], with an Le_V formulation demonstrating better agreement with measured L_b, in agreement with Bouvet et al., [49]. Consequently, it appears that for ultra-lean CH_4/H_2 blends ($\Phi < 0.70$), Le_D best depicts expected thermo-diffusive behaviour.

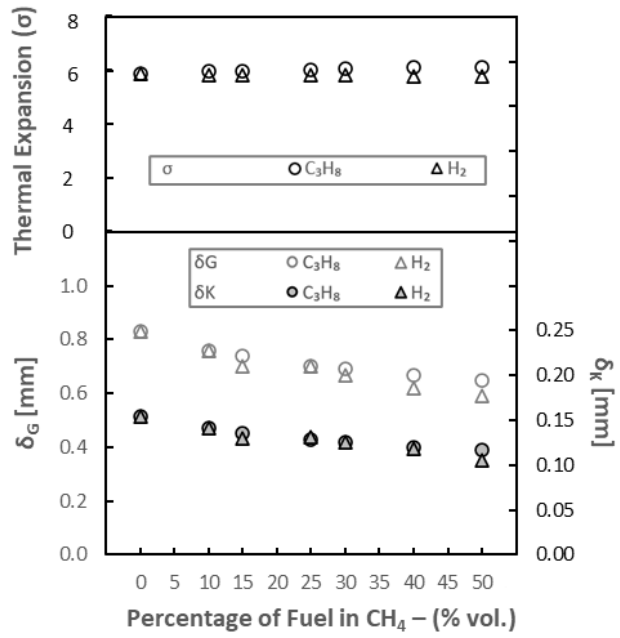

Fig. 12 – Variations in δ and σ with addition of C_3H_8 or H_2 (Φ=0.65)

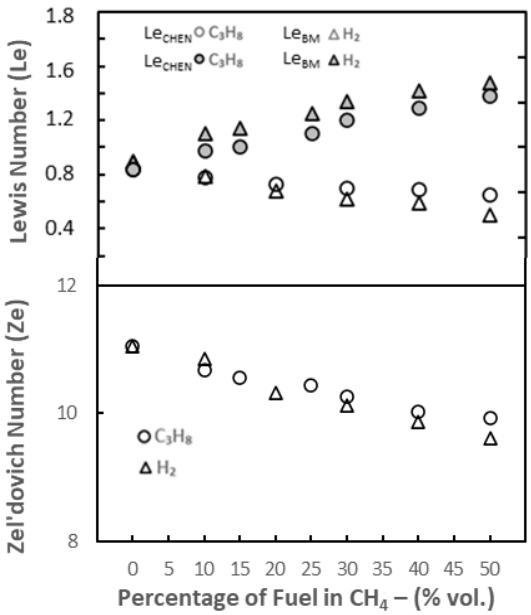

Fig. 13 – Variations in Ze and Le with addition of C_3H_8 or H_2 (Φ=0.65)

Kwon et al. [68], in their study of cellular instabilities and self-acceleration of outwardly propagating spherical flames, emphasised that the most important parameters that induce hydrodynamic and diffusional-thermal cellularities are; thermal expansion, flame thickness, non-unity Le and global activation energy (or equivalently Ze [68]). Hydrodynamic instabilities originate from the thermal expansion of gases [7], with the growth rate of hydrodynamic instability proportional to the density jump across the flame, in the limit of an infinitely thin flame propagating at a constant velocity, consistent with the hydrodynamic theory of Darrieus and Landau [7]. For outwardly propagating spherical flames, curvature induced positive stretch tends to stabilise the flame, as such the flame thickness plays a significant role, since the thinner the flame the weaker the influence of curvature, hence the risk of destabilisation is increased. It is interesting to note in Fig. 12 that in the case of the CH_4/H_2 flames, the thermal expansion remains almost constant (relative differences < 2%), whilst the flame thickness decreases, with increasing H_2 fractions (up to 50% vol.), in effect promoting hydrodynamic instabilities. With respect to the CH_4/C_3H_8, flames, the thermal expansion also remains almost constant (< 3%), with the flame thickness also decreasing with increasing C_3H_8 fraction at a similar rate as with H_2 enrichment, thereby also promoting hydrodynamic instabilities. C_3H_8 and H_2 addition to ultra-lean CH_4, however, result in the opposite L_b behaviour. The development of thermo-diffusional instabilities results from effect of non-equidiffusion, represented by Le. With respect to the CH_4/H_2 flames, the effects of preferential diffusion, are a consequence of the higher mass diffusivity of H_2 and CH_4 compared to the O_2 molecule. Since Le decreases with increasing H_2 concentration (Fig. 13), diffusional-thermal instabilities are promoted. It should be noted that the front structure of the ultra-lean CH_4/H_2 flame remained 'smooth', with some large 'cracks' appearing on the flame surface, with increasing H_2 fraction (>25%) and at large flame radii, although no cellular growth was observed. Since the development of preferential diffusional instabilities requires a modification of the flame structure, Kwon et al. [68] emphasised that it is reasonable to expect that the global activation energy (illustrated as Ze in Fig. 13), should also impact on the development of cellularity. As such, a lower E_a will tend to enhance instability of a diffusionally unstable flame, such as the CH_4/H_2 flame, with both Le and Ze decreasing with increasing H_2 content, as illustrated in Fig.

13. For lean CH_4/H_2, changes in measured L_b are thus potentially the result of the competing hydrodynamic and thermo-diffusive instabilities. However, with respect to the CH_4/C_3H_8 flames, since the mass diffusivity of C_3H_8 is lower than that of air, diffusional-thermal effects (Le > 1, see Fig. 13) seem to have the propensity of moderating hydrodynamic instabilities, yielding a stabilising influence on the flame, reflected in augmented L_b.

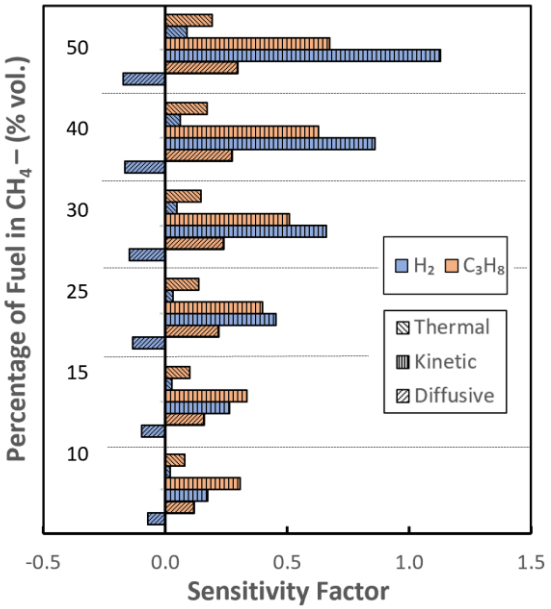

Fig. 14 – Sensitivity Analysis of U_L for CH_4/H_2 and CH_4/C_3H_8 blends, Φ=0.65

Enhancement in flame speed due to enrichment of H_2 or C_3H_8 to CH_4 can be categorised as a combination of thermal, kinetic, and diffusive effects [47,69]. The individual impact of each pathway can be modelled as per Eqn. 15:

$$U_L \sim \left(D_T \cdot Le_{eff}\right)^{1/2} exp(-T_a/2T_{ad}) \qquad \text{Eqn. (15)}$$

The first term on the right-hand side [$(D_T \cdot Le_{eff})$] reflects the diffusive influence. The second term [$exp(-T_a/2T_{ad})$], represents the Arrhenius factor, which incorporates the relative influence of the global activation energy through the activation temperature [$T_a = (E_a/R_u)$] and the adiabatic flame temperature. These individually represent the kinetic (T_a) and thermal (T_{ad}) influences on flame speed. With respect to Le formulation, it was determined from Fig. 11 that an Le_H and Le_D formulation best captured changes in thermo-diffusive behaviour for the CH_4/C_3H_8 and CH_4/H_2 blends at an Φ = 0.65, respectively. This conclusion is maintained irrespective of the theoretical relationship employed relating L_b to Le, and consequently applied for the following analysis. Eqn. 15 can be differentiated to determine the sensitivity of each individual pathway on the overall influence of the flame propagation. Thus, the overall sensitivity coefficient can be expressed as:

$$\frac{1}{U_L} \cdot \frac{dU_L}{dx} = \frac{1}{2 \cdot D_T \cdot Le} \cdot \frac{d(D_T \cdot Le)}{dx} - \frac{1}{2 \cdot T_{ad}} \cdot \frac{2 \cdot T_a}{dx} + \frac{T_a}{2 \cdot T_{ad}^2} \frac{2 \cdot T_{ad}}{dx} \qquad \text{Eqn. (16)}$$

where '*x*' is the volume fraction of either H_2 or C_3H_8 in the individual fuel blend. Note that the three terms on the right-hand side denote the influence of the diffusive, kinetic, and thermal effects, respectively. Sensitivity analysis for the blends considered is presented in Fig. 14, with a positive and

negative sensitivity factor representing flame speed enhancement and inhibition, correspondingly. For the CH_4/H_2 and CH_4/C_3H_8 blends, enhancement in flame speed is principally an Arrhenius effect (kinetic), principally through the reduction of overall activation energy and thus the activation temperature. For identical volumetric additions up to 15%, C_3H_8 blends yield a greater reduction in E_a than H_2, with H_2 having a greater influence for higher fractions, due to their molecular weights. This trend is well captured by both experimental and modelling flame speed results (Fig. 10), with H_2 addition above 30% resulting in significantly greater flame speeds than for the equivalent C_3H_8 case. With respect to the thermal pathway, its impact is modest in comparison to the kinetic effect, with the influence of the thermal pathway correlating with nominal modelled changes in adiabatic flame temperature, with C_3H_8 and H_2 addition resulting in changes in adiabatic flame temperature of < 50 K and < 25K, respectively. In terms of the diffusive pathway, C_3H_8 and H_2 result in sensitivity of similar strength, but with opposite sensitivity, consistent with their Le trends, increasing and decreasing, respectively. The conclusions drawn thus far, can be used to explain the differences in flame speeds between the ultra-lean CH_4/C_3H_8 and CH_4/H_2 blends, with up to 30% volumetric additions of C_3H_8 or H_2 resulting in similar flame enhancement of CH_4-based fuels, and H_2 having greater influence for higher fractions. It should be noted however, that conclusions should be taken qualitatively rather than from a quantitative perspective, given there exists several different theoretical formulations to evaluate the same fundamental property (e.g. E_a, see Section 4.1). Furthermore, differences are to be expected by applying different reaction mechanisms, due to the number of identical reactions within each mechanism that have different associated Arrhenius coefficients [70]. However, it is noted that qualitative trends should remain valid, and thus performing such sensitivity analysis from first principles remains relevant providing useful insights.

5.4 Tertiary Natural Gas and Hydrogen Blends

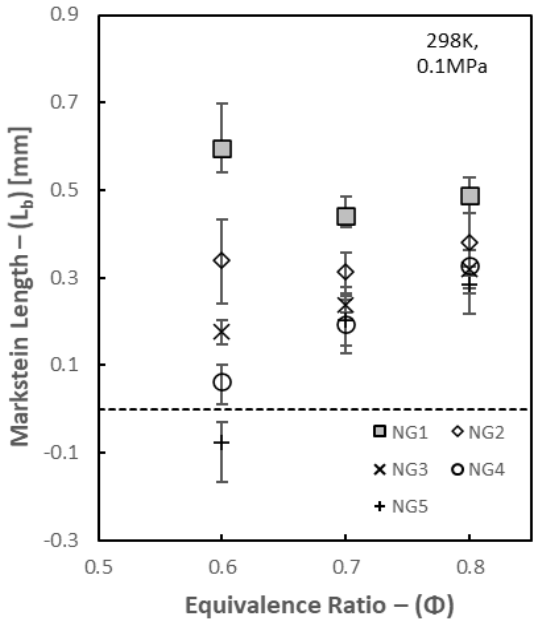

Fig. 15 – Measured L_b for various NG for selected NG compositions

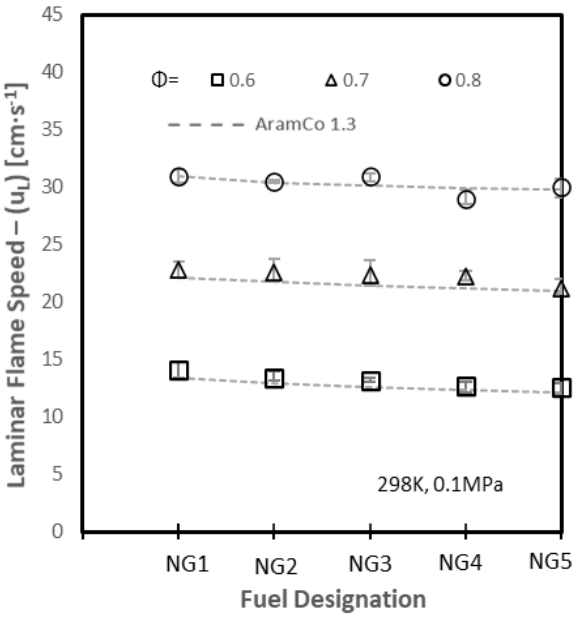

Fig. 16 – Measured and Modelled U_L values for selected NG compositions

Having examined and quantified the lean combustion characteristics of C_{1-4} alkanes and binary blends of CH_4/C_3H_8 and CH_4/H_2, an understanding of the impact of tertiary blends was considered. Plausible short-term variations in hydrogen-enriched multi-component natural gas (NG)

flame combustion characteristics were experimentally and numerically investigated, with compositions of mixtures detailed in Table 1.

Measured L_b of NG/H_2 blends are illustrated in Fig. 15. Evidently, at the richest conditions (Φ=0.80), L_b behaviour is consistent with that previously measured for pure CH_4, C_3H_8 and CH_4/C_3H_8 binary mixtures (see Fig. 4), with H_2 (15% by vol.) yielding nominal influence on flame stability characteristics (positive L_b, Le > 1) as expected. However, significant changes in flame behaviour are observable at leaner conditions, with small variations in NG composition (CH_4:C_3H_8 molar ratio) discernibly influencing flame-stretch propagation characteristics, with NG1 and NG5 containing the largest fractions of C_3H_8 and CH_4, respectively, behaving in analogous manner to that of pure C_3H_8 (positive L_b) and CH_4 (negative L_b) at Φ=0.60 (see Fig.4). From a preferential-diffusional perspective, H_2 and C_3H_8 promote opposite lean CH_4 based flame stability behaviour, with the influence of H_2 prominent for NG 3 – 5, which exhibit decreasing L_b as conditions get leaner. NG5, the blend containing the highest fraction of CH_4 (lowest C_3H_8 fraction), is observed to display a negative L_b, indicating an acceleration of the flame with stretch, behaviour equivalent to results presented for 100% CH_4 and CH_4/H_2 (85/15%, Φ=0.60, Fig 4). Conversely, NG1 exhibits increasing L_b as Φ decreases, with the influence of H_2 counteracted by the higher fraction of C_3H_8. Khan et al., [19], measured L_b for various H_2-enriched NG ($CH_4/C_2H_6/C_3H_8$) compositions, showing a reduction in L_b with decreasing heavier hydrocarbon fraction for a fixed volumetric H_2 addition, in good agreement with trends illustrated in Fig. 15.

Fig. 16 presents the measured laminar burning velocities of the NG/H_2 mixtures (Φ=0.6 – 0.8), with lines representing modelled values using the Aramco 1.3 mechanism. Generally, a marginal decrease in U_L is measured with decreasing C_3H_8 fraction (NG 1→NG 5), with leanest flames most prominently affected. As can be seen, this trend very well captured by the Aramco 1.3 reaction mechanism. At equivalent Φ, the previously tested binary blends (CH_4/H_2 & CH_4/C_3H_8 [85/15% vol.]), CH_4-based fuels exhibited equivalently enhanced reactivity at leanest conditions, upon H_2 or C_3H_8 addition, in good agreement with U_L values observed for the tested NG blends.

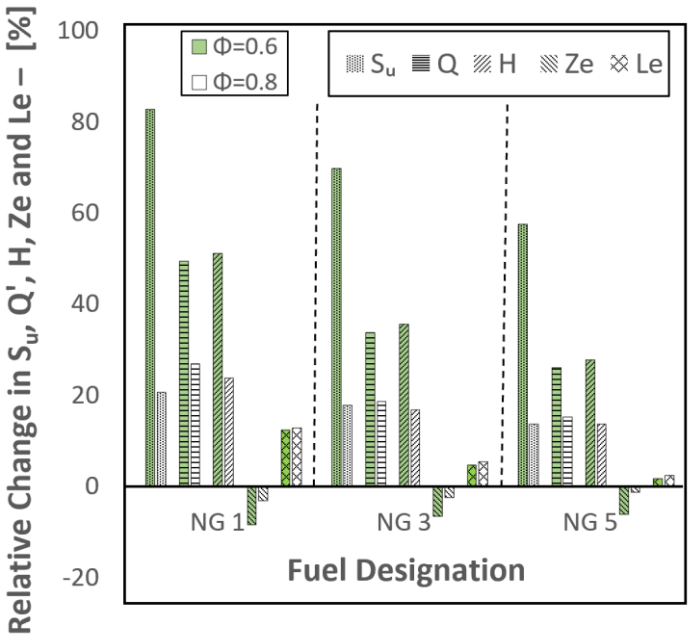

Fig. 17 – Relative changes, normalised to pure CH_4, in S_u, Q', H radical, Ze and Le between NG 1 – 3 – 5, at Φ=0.60 & 0.80

The sensitivity analysis performed in Section 5.3 (see Fig. 14), concluded that observed augmentations in flame propagation of ultra-lean (Φ=0.65) CH_4/H_2 and CH_4/C_3H_8 (up to 50% vol.) was principally an Arrhenius effect, through the reduction of the global activation energy. Consistent with modelling details described earlier (Section 5.2), Fig. 17 depicts relative changes in global activation energy (through Ze), normalised to that of pure CH_4, for NG1 (lowest CH_4 content), NG3, and NG5 (highest CH_4 content), for Φ=0.60 and 0.80, alongside modelled relative changes in unstretched flame speed (S_u), volumetric heat release rates (Q'), concentration of mole fractions of H radicals, and effective Lewis Number (Le_{eff}). Evidently, at the leanest conditions, NG compositions with the highest C_3H_8 content (NG 1) display greatest reduction in Ze (E_a), consistent with enhanced augmentation in measured S_u. It is noted that the relative changes in adiabatic flame temperature exhibited by the NG blends are negligible (<2%), irrespective of Φ specified, re-affirming that changes in attained laminar flame speeds are principally kinetic in nature and not thermal. Since all NG compositions tested contain equal volumetric H_2 fractions, changes in E_a are principally related to variations in CH_4:C_3H_8 content. Furthermore, as previously discussed, H_2 and C_3H_8 fuels display higher heat of combustion per mass than CH_4, hence measured changes in flame speed are directly correlated to changes in Q', with production of key radicals, notably H, influencing CH_4 oxidation mechanisms. As expected, NG blends containing the highest volumetric concentrations of C_3H_8 for a fixed H_2 enrichment level (15% by vol.) yield greatest augmentations in modelled Q', with enhancement promoted with decreasing Φ, as illustrated in Fig. 17. The same trend exists with respect to predicted H radical production concentrations, in good agreement with measured U_L trends.

Conclusions

The influence of changing Le on-flame behaviour of lean CH_4, CH_4/C_3H_8 and CH_4/H_2, and H_2-enriched natural gas mixtures has been investigated in detail, employing the spherically expanding flame configuration to measure flame speed and corresponding Markstein length. From this work the following can be concluded:

- Equal volumetric additions of either H_2 and C_3H_8 to CH_4 flames (up to 30% by vol.) result in similar enhancement of burning rate with opposing susceptibility to preferential diffusional instability. It is noted the influence of H_2 and C_3H_8 yield greatest influence at leanest conditions, a reflection of each individual fuels' Le behaviour. At a fixed equivalence ratio of 0.65, limited changes in composition provide a marked change in the premixed flame response with the addition of C_2H_6 and C_3H_8 to CH_4, with L_b plateauing clearly identifiable for C_2H_6, less so for C_3H_8.
- A diffusional based Lewis Number formulation (Le_D) yielded best correlation with measured stretch related behaviour of lean (Φ ≤ 0.7) CH_4/H_2 mixtures containing up to 50% H_2, whilst a heat-release model (Le_H) resulted in better agreement with lean CH_4/C_3H_8 mixtures, with the formulation linking Le to L_b proposed by Bechtold and Matalon resulting in good quantitative and qualitative agreement.
- Modelling studies suggest that measured augmentations in flame propagation of ultra-lean CH_4-based fuels upon H_2 or C_3H_8 addition is predominantly a consequence of enhanced production of key radicals, notably H, facilitating CH_4 oxidation mechanics, with C_3H_8 yielding a greater influence than H_2 for equal volumetric fractions.
- A sensitivity analysis related to the major flame enhancing pathways (thermal, kinetic, diffusive) has shown that enhanced flame propagation of lean CH_4/H_2 and CH_4/C_3H_8, is principally an Arrhenius effect (kinetic), predominantly through the reduction of the activation temperature. The diffusive pathway was comparable in strength for both blends, but with opposite sensitivities, consistent with their respective Le trends.

- Changes in measured L_b behaviour of lean hydrogen enriched natural gas (for a fixed volumetric H_2 fraction, 15% vol.) result from variations in fuel composition, with blends containing lowest and highest heavier hydrocarbon content exhibiting analogous stretch-related behaviour to that of pure CH_4 and C_3H_8, due to preferential-diffusional preferences. Greatest relative changes in flame speed due to variations in heavier hydrocarbon content of the chosen natural gas-hydrogen blends were observed at leanest conditions. Modelling suggests that flame speed changes are principally linked to a reduction in activation energy (kinetic), with differences corresponding to variations in volumetric heat release rates and production of key radicals.

References

[1] Dirrenberger P, Gall L, Bounaceur R, Herbinet O, Glaude PA, Konnov A, et al. Measurements of Laminar Flame Velocity for Components of Natural Gas. Energy and Fuels 2011;25:3875–84.

[2] Lowry W, Vries J De, Krejci M, Petersen E, Metcalfe W. Measurements and Modeling of Pure Alkanes and Alkane Blends 2014;133:1–9.

[3] Morones A, Ravi S, Plichta D, Petersen EL, Donohoe N, Heufer A, et al. Laminar and turbulent flame speeds for natural gas/hydrogen blends. Proc ASME Turbo Expo 2014;4B:1–8.

[4] Abbott DJ, Bowers JP, James SR. The Impact of Natural Gas Composition Variations on the Operation of Gas Turbines for Power Generation. Futur Gas Turbine Technol 2012:1.

[5] Taamallah S, Vogiatzaki K, Alzahrani FM, Mokheimer EMA, Habib MA, Ghoniem AF. Fuel flexibility, stability and emissions in premixed hydrogen-rich gas turbine combustion: Technology, fundamentals, and numerical simulations. Appl Energy 2015;154:1020–47.

[6] Lipatnikov AN, Chomiak J. Molecular transport effects on turbulent flame propagation and structure. Prog Energy Combust Sci 2005;31:1–73.

[7] Law CK. Combustion Physics. 1st ed. Cambridge University Press; 2006.

[8] Muppala SPR, Nakahara M, Aluri NK, Kido H, Wen JX, Papalexandris M V. Experimental and analytical investigation of the turbulent burning velocity of two-component fuel mixtures of hydrogen, methane and propane. Int J Hydrogen Energy 2009;34:9258–65.

[9] Aldredge RC, Killingsworth NJ. Experimental evaluation of Markstein-number influence on thermoacoustic instability. Combust Flame 2004;137:178–97.

[10] Bell JB, Cheng RK, Day MS, Shepherd IG. Numerical simulation of Lewis number effects on lean premixed turbulent flames. Proc Combust Inst 2007;31 I:1309–17.

[11] Brower M, Petersen EL, Metcalfe W, Curran HJ, Füri M, Bourque G, et al. Ignition delay time and laminar flame speed calculations for natural gas/hydrogen blends at elevated pressures. J Eng Gas Turbines Power 2013;135:1–10.

[12] Chakraborty N, Cant RS. Effects of Lewis number on turbulent scalar transport and its modelling in turbulent premixed flames. Combust Flame 2009;156:1427–44.

[13] Savard B, Blanquart G. An a priori model for the effective species Lewis numbers in premixed turbulent flames. Combust Flame 2014;161:1547–57.

[14] Dinkelacker F, Manickam B, Muppala SPR. Modelling and simulation of lean premixed turbulent methane/hydrogen/air flames with an effective Lewis number approach. Combust Flame 2011;158:1742–9.

[15] Dagaut P, Dayma G. Hydrogen-enriched natural gas blend oxidation under high-pressure conditions: Experimental and detailed chemical kinetic modeling. Int J Hydrogen Energy 2006;31:505–15.

[16] Huang Z, Zhang Y, Zeng K, Liu B, Wang Q, Jiang D. Measurements of laminar burning velocities for natural gas-hydrogen-air mixtures. Combust Flame 2006;146:302–11.

[17] Miao H, Jiao Q, Huang Z, Jiang D. Effect of initial pressure on laminar combustion characteristics of hydrogen enriched natural gas. Int J Hydrogen Energy 2008;33:3876–85.

[18] Nilsson EJK, van Sprang A, Larfeldt J, Konnov AA. The comparative and combined effects of

hydrogen addition on the laminar burning velocities of methane and its blends with ethane and propane. Fuel 2017;189:369–76.
[19] Khan AR, Ravi MR, Ray A. Experimental and chemical kinetic studies of the effect of H 2 enrichment on the laminar burning velocity and flame stability of various multicomponent natural gas blends. Int J Hydrogen Energy 2019;44:1192–212.
[20] Pugh D. Combustion characterisation of compositionally dynamic steelworks gases. Cardiff University, 2013.
[21] Zitouni SEM. Combustion Characteristics of Lean Premixed Methane/Higher Hydrocarbon/Hydrogen Flames. Cardiff University, 2020.
[22] Pugh DG, Crayford AP, Bowen PJ, Al-Naama M. Parametric investigation of water loading on heavily carbonaceous syngases. Combust Flame 2016;164:126–36.
[23] Law CK, Jomaas G, Bechtold JK. Cellular instabilities of expanding hydrogen/propane spherical flames at elevated pressures: Theory and experiment. Proc Combust Inst 2005;30:159–67.
[24] Giannakopoulos GK, Gatzoulis A, Frouzakis CE, Matalon M, Tomboulides AG. Consistent definitions of “Flame Displacement Speed” and “Markstein Length” for premixed flame propagation. Combust Flame 2015;162:1249–64.
[25] Bradley D, Gaskell PH, Gu XJ. Burning velocities, Markstein lengths, and flame quenching for spherical methane-air flames: A computational study. Combust Flame 1996;104:176–98.
[26] Chen Z, Burke MP, Ju Y. Effects of Lewis number and ignition energy on the determination of laminar flame speed using propagating spherical flames. Proc Combust Inst 2009;32 I:1253–60.
[27] Burke MP, Chen Z, Ju Y, Dryer FL. Effect of cylindrical confinement on the determination of laminar flame speeds using outwardly propagating flames. Combust Flame 2009;156:771–9.
[28] Chen Z. On the accuracy of laminar flame speeds measured from outwardly propagating spherical flames: Methane/air at normal temperature and pressure. Combust Flame 2015;162:2442–53.
[29] Verhelst S, Woolley R, Lawes M, Sierens R. Laminar and unstable burning velocities and Markstein lengths of hydrogen-air mixtures at engine-like conditions. Proc Combust Inst 2005;30:209–16.
[30] Gu XJ, Haq MZ, Lawes M, Woolley R. Laminar burning velocity and Markstein lengths of methane-air mixtures. Combust Flame 2000;121:41–58.
[31] Halter F, Tahtouh T, Mounaïm-Rousselle C. Nonlinear effects of stretch on the flame front propagation. Combust Flame 2010;157:1825–32.
[32] Wu CK, Law CK. On the determination of laminar flame speeds from stretched flames. Symp Combust 1985;20:1941–9.
[33] Taylor SC. Burning velocity and the influence of flame stretch. University of Leeds, 1991.
[34] Dowdy DR, Smith DB, Taylor SC, Williams A. The use of expanding spherical flames to determine burning velocities and stretch effects in hydrogen/air mixtures. Symp Combust 1991;23:325–32.
[35] Frankel ML, Sivashinsky GI. On effects due to thermal expansion and lewis number in spherical flame propagation. Combust Sci Technol 1983;31:131–8.
[36] Markstein GH. Experimental and Theoretical Studies of Flame-Front Stability. J Aeronaut Sci 1951;18:199–209.
[37] Chen Z. On the extraction of laminar flame speed and Markstein length from outwardly propagating spherical flames. Combust Flame 2011;158:291–300.
[38] Wu F, Liang W, Chen Z, Ju Y, Law CK. Uncertainty in stretch extrapolation of laminar flame speed from expanding spherical flames. Proc Combust Inst 2015;35:663–70.
[39] Lapalme D, Lemaire R, Seers P. Assessment of the method for calculating the Lewis number of H2/CO/CH4 mixtures and comparison with experimental results. Int J Hydrogen Energy 2017;42:8314–28.
[40] Kelley AP, Law CK. Nonlinear effects in the extraction of laminar flame speeds from expanding

spherical flames. Combust Flame 2009;156:1844–51.
[41] Ronney PD, Sivashinsky GI. A Theoretical Study of Propagation and Extinction of Nonsteady Spherical Flame Fronts. SIAM J Appl Math 1989;49:1029–46.
[42] Metcalfe WK, Burke SM, Ahmed SS, Curran HJ. A hierarchical and comparative kinetic modeling study of C1 - C2 hydrocarbon and oxygenated fuels. Int J Chem Kinet 2013;45:638–75.
[43] Bechtold JK, Matalon M. The dependence of the Markstein length on stoichiometry. Combust Flame 2001;127:1906–13.
[44] Egolfopoulos FN, Law CK. Chain mechanisms in the overall reaction orders in laminar flame propagation. Combust Flame 1990;80:7–16.
[45] Sun CJ, Sung CJ, He L, Law CK. Dynamics of weakly stretched flames: Quantitative description and extraction of global flame parameters. Combust Flame 1999;118:108–28.
[46] Kumar K, Sung CJ. Laminar flame speeds and extinction limits of preheated n-decane/O2/N2 and n-dodecane/O2/N2 mixtures. Combust Flame 2007;151:209–24.
[47] Ravi S, Sikes TG, Morones A, Keesee CL, Petersen EL. Comparative study on the laminar flame speed enhancement of methane with ethane and ethylene addition. Proc Combust Inst 2015;35:679–86.
[48] Jomaas G, Law CK, Bechtold JK. On transition to cellularity in expanding spherical flames. J Fluid Mech 2007;583:1–26.
[49] Bouvet N, Halter F, Chauveau C, Yoon Y. On the effective Lewis number formulations for lean hydrogen/hydrocarbon/ air mixtures. Int J Hydrogen Energy 2013;38:5949–60.
[50] Hu E, Huang Z, He J, Miao H. Experimental and numerical study on laminar burning velocities and flame instabilities of hydrogen-air mixtures at elevated pressures and temperatures. Int J Hydrogen Energy 2009;34:8741–55.
[51] Tang C, Huang Z, Jin C, He J, Wang J, Wang X, et al. Laminar burning velocities and combustion characteristics of propane-hydrogen-air premixed flames. Int J Hydrogen Energy 2008;33:4906–14.
[52] Tang C, Huang Z, Wang J, Zheng J. Effects of hydrogen addition on cellular instabilities of the spherically expanding propane flames. Int J Hydrogen Energy 2009;34:2483–7.
[53] Poling BE, Prausnitz JM, O'Connell JP. The properties of gases and liquids. 5th ed. McGraw-Hill; 2001.
[54] Fairbanks DF, Wilke CR. Diffusion Coefficients in Multicomponent Gas Mixtures. Ind Eng Chem 1950;42:471–5.
[55] Dandy D. Transport Properties Calculator n.d. http://navier.engr.colostate.edu/code/code-2/index.html (accessed January 31, 2020).
[56] Hassan MI, Aung KT, Faeth GM. Measured and predicted properties of laminar premixed methane/air flames at various pressures. Combust Flame 1998;115:539–50.
[57] Chen Z, Qin X, Ju Y, Zhao Z, Chaos M, Dryer FL. High temperature ignition and combustion enhancement by dimethyl ether addition to methane-air mixtures. Proc Combust Inst 2007;31 I:1215–22.
[58] Tahtouh T, Halter F, Mounaïm-Rousselle C. Measurement of laminar burning speeds and Markstein lengths using a novel methodology. Combust Flame 2009;156:1735–43.
[59] Law CK, Sung CJ. Structure, aerodynamics, and geometry of premixed flamelets. Prog Energy Combust Sci 2000;26:459–505.
[60] Jomaas G, Zheng XL, Zhu DL, Law CK. Experimental determination of counterflow ignition temperatures and laminar flame speeds of C2-C3 hydrocarbons at atmospheric and elevated pressures. Proc Combust Inst 2005;30:193–200.
[61] Konnov AA, Mohammad A, Kishore VR, Kim N Il, Prathap C, Kumar S. A comprehensive review of measurements and data analysis of laminar burning velocities for various fuel+air mixtures. Prog Energy Combust Sci 2018;68:197–267.
[62] Hawkes ER, Chen JH. Direct numerical simulation of hydrogen-enriched lean premixed methane–air flames. Combust Flame 2004;138:242–58.

[63] Wang H, You X, Joshi A V, Davis SG, Laskin A, Egolfopoulos F, et al. USC Mech Version II. High-temperature combustion reaction model of H2/CO/C1-C4 compounds. Combust Kinet Lab Univ South California, Los Angeles, CA, Accessed Aug 2007.
[64] Smith G, Golden D, Frenklach M, Moriarty N, Eitneer B. GRI-Mech 3.0 n.d. http://www.me.berkeley.edu/gri_mech.
[65] Mechanical and Aerospace Engineering (Combustion Research) University of California at San Diego. Chemical-Kinetic Mechanisms for Combustion Applications n.d. http://combustion.ucsd.edu.
[66] Hu E, Huang Z, He J, Jin C, Zheng J. Experimental and numerical study on laminar burning characteristics of premixed methane-hydrogen-air flames. Int J Hydrogen Energy 2009;34:4876–88.
[67] Tan Y, Dagaut P, Cathonnet M, Boettner JC. Oxidation and ignition of Methane-Propane and Methane-Ethane-Propane mixtures: Experiments and modeling. Combust Sci Technol 1994;103:133–51.
[68] Kwon OC, Rozenchan G, Law CK. Cellular instabilities and self-acceleration of outwardly propagating spherical flames. Proc Combust Inst 2002;29:1775–83.
[69] Tang CL, Huang ZH, Law CK. Determination, correlation, and mechanistic interpretation of effects of hydrogen addition on laminar flame speeds of hydrocarbon-air mixtures. Proc Combust Inst 2011;33:921–8.
[70] Hu E, Chen Y, Zhang Z, Li X, Cheng Y, Huang Z. Experimental study on ethane ignition delay times and evaluation of chemical kinetic models. Energy and Fuels 2015;29:4557–66.